

Prediction of protein function using a deep convolutional neural network ensemble

Evangelia I. Zacharaki

Center for Visual Computing, CentraleSupélec and GALEN Team, INRIA Saclay, France

ABSTRACT

Background. The availability of large databases containing high resolution three-dimensional (3D) models of proteins in conjunction with functional annotation allows the exploitation of advanced supervised machine learning techniques for automatic protein function prediction.

Methods. In this work, novel shape features are extracted representing protein structure in the form of local (per amino acid) distribution of angles and amino acid distances, respectively. Each of the multi-channel feature maps is introduced into a deep convolutional neural network (CNN) for function prediction and the outputs are fused through support vector machines or a correlation-based k-nearest neighbor classifier. Two different architectures are investigated employing either one CNN per multi-channel feature set, or one CNN per image channel.

Results. Cross validation experiments on single-functional enzymes ($n = 44,661$) from the PDB database achieved 90.1% correct classification, demonstrating an improvement over previous results on the same dataset when sequence similarity was not considered.

Discussion. The automatic prediction of protein function can provide quick annotations on extensive datasets opening the path for relevant applications, such as pharmacological target identification. The proposed method shows promise for structure-based protein function prediction, but sufficient data may not yet be available to properly assess the method's performance on non-homologous proteins and thus reduce the confounding factor of evolutionary relationships.

Submitted 10 August 2016

Accepted 11 June 2017

Published 17 July 2017

Corresponding author

Evangelia I. Zacharaki,
evangelia.zacharaki@centralesupelec.fr

Academic editor

James Procter

Additional Information and
Declarations can be found on
page 14

DOI 10.7717/peerj-cs.124

© Copyright
2017 Zacharaki

Distributed under
Creative Commons CC-BY 4.0

OPEN ACCESS

Subjects Bioinformatics, Computational Biology, Data Mining and Machine Learning

Keywords Enzyme classification, Function prediction, Deep learning, Convolutional neural networks, Structure representation

INTRODUCTION

Metagenomics has led to a huge increase of protein databases and the discovery of new protein families ([Godzik, 2011](#)). While the number of newly discovered, but possibly redundant, protein sequences rapidly increases, experimentally verified functional annotation of whole genomes remains limited. Protein structure, i.e., the 3D configuration of the chain of amino acids, is a very good predictor of protein function, and in fact a more reliable predictor than protein sequence because it is far more conserved in nature ([Illergård, Ardell & Elofsson, 2009](#)).

By now, the number of proteins with functional annotation and experimentally predicted structure of their native state (e.g., by NMR spectroscopy or X-ray

crystallography) is adequately large to allow machine learning models to be trained that will be able to perform automatic functional annotation of unannotated proteins (Amidi *et al.*, 2017). Also, as the number of protein sequences rapidly grows, the overwhelming majority of proteins can only be annotated computationally. In this work enzymatic structures from the Protein Data Bank (PDB) are considered and the enzyme commission (EC) number is used as a fairly complete framework for annotation. The EC number is a numerical classification scheme based on the chemical reactions the enzymes catalyze, proven by experimental evidence (Webb, 1992).

There have been plenty machine learning approaches in the literature for automatic enzyme annotation. A systematic review on the utility and inference of various computational methods for functional characterization is presented in *Sharma & Garg (2014)*, while a comparison of machine learning approaches can be found in *Yadav & Tiwari (2015)*. Most methods use features derived from the amino acid sequence and apply support vector machines (SVM) (Cai *et al.*, 2003; Han *et al.*, 2004; Dobson & Doig, 2005; Chen *et al.*, 2006; Zhou *et al.*, 2007; Lu *et al.*, 2007; Lee *et al.*, 2009; Qiu *et al.*, 2010; Wang *et al.*, 2010; Wang *et al.*, 2011; Amidi *et al.*, 2016), k-nearest neighbor (kNN) classifier (Huang *et al.*, 2007; Shen & Chou, 2007; Nasibov & Kandemir-Cavas, 2009), classification trees/forests (Lee *et al.*, 2009; Kumar & Choudhary, 2012; Nagao, Nagano & Mizuguchi, 2014; Yadav & Tiwari, 2015), and neural networks (Volpato, Adelfio & Pollastri, 2013). In *Borgwardt *et al.* (2005)* sequential, structural and chemical information was combined into one graph model of proteins which was further classified by SVM. However, there has been little work in the literature on automatic enzyme annotation based only on structural information. A Bayesian approach (Borro *et al.*, 2006) for enzyme classification using structure derived properties achieved 45% accuracy. Amidi *et al.* (2016) obtained 73.5% classification accuracy on 39,251 proteins from the PDB database when they used only structural information.

In the past few years, deep learning techniques, and particularly convolutional neural networks, have rapidly become the tool of choice for tackling many challenging computer vision tasks, such as image classification (Krizhevsky, Sutskever & Hinton, 2012). The main advantage of deep learning techniques is the automatic exploitation of features and tuning of performance in a seamless fashion, that simplifies the conventional image analysis pipelines. CNNs have recently been used for protein secondary structure prediction (Spencer, Eickholt & Cheng, 2015; Li & Shibuya, 2015). In *Spencer, Eickholt & Cheng (2015)* prediction was based on the position-specific scoring matrix profile (generated by PSI-BLAST), whereas in *Li & Shibuya (2015)* 1D convolution was applied on features related to the amino acid sequence. Also, a deep CNN architecture was proposed in *Lin, Lanchantin & Qi (2016)* to predict protein properties. This architecture used a multilayer shift-and-stitch technique to generate fully dense per-position predictions on protein sequences. To the best of the author's knowledge, deep CNNs have not been used for prediction of protein function so far.

In this work the author exploits experimentally acquired structural information of enzymes and apply deep learning techniques in order to produce models that predict enzymatic function based on structure. Novel geometric descriptors are introduced and the efficacy of the approach is illustrated by classifying a dataset of 44,661 enzymes from

the PDB database into the $l = 6$ primary categories: oxidoreductases (EC1), transferases (EC2), hydrolases (EC3), lyases (EC4), isomerases (EC5), ligases (EC6). The novelty of the proposed method lies first in the representation of the 3D structure as a “bag of atoms (amino acids)” which are characterized by geometric properties, and secondly in the exploitation of the extracted feature maps by deep CNNs. Although assessed for enzymatic function prediction, the method is not based on enzyme-specific properties and therefore can be applied (after re-training) for automatic large-scale annotation of other 3D molecular structures, thus providing a useful tool for data-driven analysis. In the following sections more details on the implemented framework are first provided, including the representation of protein structure, the CNN architecture and the fusion process of the network outputs. Then the evaluation framework and the obtained results are presented, followed by some discussion and conclusions.

METHODS

Data-driven CNN models tend to be domain agnostic and attempt to learn additional feature bases that cannot be represented through any handcrafted features. It is hypothesized that by combining “amino acid specific” descriptors with the recent advances in deep learning we can boost model performance. The main advantage of the proposed method is that it exploits complementarity in both data representation phase and learning phase. Regarding the former, the method uses an enriched geometric descriptor that combines local shape features with features characterizing the interaction of amino acids on this 3D spatial model. Shape representation is encoded by the local (per amino acid type) distribution of torsion angles ([Bermajo, Clore & Schwieters, 2012](#)). Amino acid interactions are encoded by the distribution of pairwise amino acid distances. While the torsion angles and distance maps are usually calculated and plotted for the whole protein ([Bermajo, Clore & Schwieters, 2012](#)), in the current approach they are extracted for each amino acid type separately, therefore characterizing local interactions. Thus, the protein structure is represented as a set of multi-channel images which can be introduced into any machine learning scheme designed for fusing multiple 2D feature maps. Moreover, it should be noted that the utilized geometric descriptors are invariant to global translation and rotation of the protein, therefore previous protein alignment is not required.

Our method constructs an ensemble of deep CNN models that are complementary to each other. The deep network outputs are combined and introduced into a correlation-based kNN classifier for function prediction. For comparison purposes, support vector machines were also implemented for final classification. Two system architectures are investigated in which the multiple image channels are considered jointly or independently, as will be described next. Both architectures use the same CNN structure (within the highlighted boxes) which is illustrated in [Fig. 1](#).

Representation of protein structure

The building blocks of proteins are amino acids which are linked together by peptide bonds into a chain. The polypeptide folds into a specific conformation depending on the interactions between its amino acid side chains which have different chemistries.

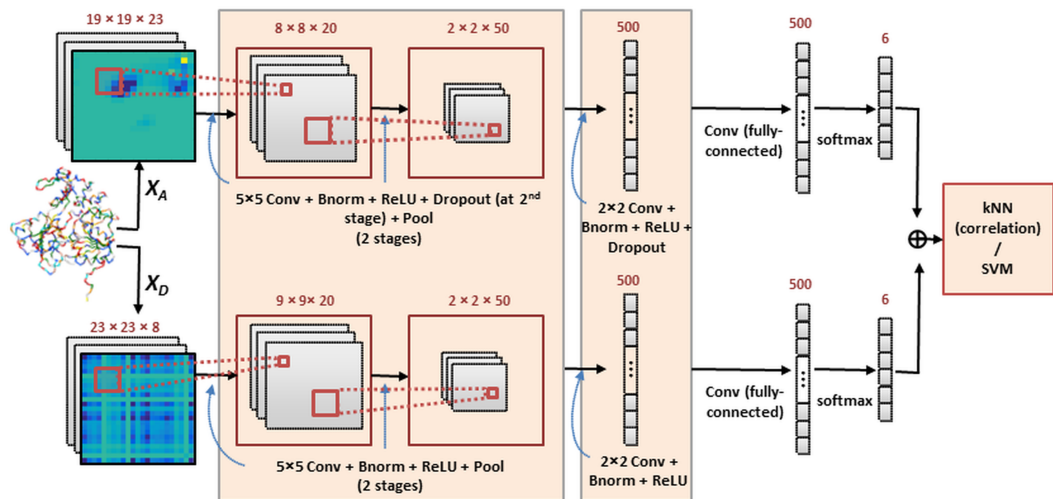


Figure 1 The deep CNN ensemble for protein classification. In this framework (*Architecture 1*) each multi-channel feature set is introduced to a CNN and results are combined by kNN or SVM classification. The network includes layers performing convolution (Conv), batch normalization (Bnorm), rectified linear unit (ReLU) activation, dropout (optionally) and max-pooling (Pool). Details are provided in ‘Classification by deep CNNs’.

Many conformations of this chain are possible due to the rotation of the chain about each carbon ($C\alpha$) atom. For structure representation, two sets of feature maps were used. They express the shape of the protein backbone and the distances between the protein building blocks (amino acids). The use of global rotation and translation invariant features is preferred over features based on the Cartesian coordinates of atoms, in order to avoid prior protein alignment, which is a bottleneck in the case of large datasets with proteins of several classes (unknown reference template space). The feature maps were extracted for every amino acid being present in the dataset including the 20 standard amino acids, as well as asparagine/aspartic (ASX), glutamine/glutamic (GLX), and all amino acids with unidentified/unknown residues (UNK), resulting in $m = 23$ amino acids in total.

Torsion angles density

The shape of the protein backbone was expressed by the two torsion angles of the polypeptide chain which describe the rotations of the polypeptide backbone around the bonds between $N-C\alpha$ (angle ϕ) and $C\alpha-C$ (angle ψ). All amino acids in the protein were grouped according to their type and the density of the torsion angles ϕ and ψ ($\in [-180, 180]$) was estimated for each amino acid type based on the 2D sample histogram of the angles (also known as Ramachandran diagram) using equally sized bins (number of bins $h_A = 19$). The histograms were not normalized by the number of instances, therefore their values indicate the frequency of each amino acid within the polypeptide chain. In the obtained feature maps (X_A), with dimensionality $[h_A \times h_A \times m]$, the number of amino acids (m) corresponds to the number of channels. Smoothness in the density function was achieved by moving average filtering, i.e., by convoluting the density map with a 2D Gaussian kernel ($\sigma = 0.5$).

Density of amino acid distances

For each amino acid $a_i, i = 1, \dots, m$, distances to amino acid $a_j, j = 1, \dots, m$, in the protein are calculated based on the coordinates of the $\text{C}\alpha$ atoms for the residues and stored as an array d_{ij} . Since the size of the proteins varies significantly, the length of the array d_{ij} is different across proteins, thus not directly comparable. In order to standardize measurements, the sample histogram of d_{ij} is extracted (using equally sized bins) and smoothed by convolution with a 1D Gaussian kernel ($\sigma = 0.5$). The processing of all pairs of amino acids resulted in feature maps (X_D) of dimension $[m \times m \times h_D]$, where $h_D = 8$ is the number of histogram bins (considered as number of channels in this case).

Classification by deep CNNs

Feature extraction stage of each CNN

The CNN architecture employs three computational blocks of consecutive convolutional, batch normalization, rectified linear unit (ReLU) activation, dropout (optionally) and max-pooling layers, and a fully-connected layer. The convolutional layer computes the output of neurons that are connected to local regions in the input in order to extract local features. It applies a 2D convolution between each of the input channels and a set of filters. The 2D activation maps are calculated by summing the results over all channels and then stacking the output of each filter to produce the output 3D volume. Batch normalization normalizes each channel of the feature map by averaging over spatial locations and batch instances. The ReLU layer applies an element-wise activation function, such as the $\max(0, x)$ thresholding at zero. The dropout layer is used to randomly drop units from the CNN during training to reduce overfitting. Dropout was used only for the X_A feature set. The pooling layer performs a downsampling operation along the spatial dimensions in order to capture the most relevant global features with fixed length. The \max operator was applied within a $[2 \times 2]$ neighborhood. The last layer is fully-connected and represents the class scores.

Training and testing stage of each CNN

The output of each CNN is a vector of probabilities, one for each of the l possible enzymatic classes. The CNN performance can be measured by a loss function which assigns a penalty to classification errors. The CNN parameters are learned to minimize this loss averaged over the annotated (training) samples. The *softmax* loss function (i.e., the *softmax* operator followed by the *logistic loss*) is applied to predict the probability distribution over categories. Optimization was based on an implementation of stochastic gradient descent. At the testing stage, the network outputs after *softmax* normalization are used as class probabilities.

Fusion of CNN outputs using two different architectures

Two fusion strategies were implemented. In the first strategy (*Architecture 1*) the two feature sets, X_A and X_D , are each introduced into a CNN, which performs convolution at all channels, and then the l class probabilities produced for each feature set are combined into a feature vector of length $l * 2$. In the second strategy (*Architecture 2*), each one of the ($m = 23$ or $h_D = 8$) channels of each feature set is introduced independently into a CNN and the obtained class probabilities are concatenated into a vector of $l * m$ features for X_A .

Table 1 Cross-validation accuracy (in percentage) in predicting main enzymatic function using the deep CNN ensemble.

| Class | Samples | Architecture 1 | | Architecture 2 | |
|--------------|---------|----------------|------|----------------|-------------|
| | | Linear-SVM | kNN | Linear-SVM | kNN |
| EC1 | 8,075 | 86.4 | 88.8 | 91.2 | 90.6 |
| EC2 | 12,739 | 84.0 | 87.5 | 88.0 | 91.7 |
| EC3 | 17,024 | 88.7 | 91.3 | 89.6 | 94.0 |
| EC4 | 3,114 | 79.4 | 78.4 | 84.9 | 80.7 |
| EC5 | 1,905 | 69.5 | 68.6 | 79.6 | 77.0 |
| EC6 | 1,804 | 61.0 | 60.6 | 73.6 | 70.4 |
| Total | 44,661 | 84.4 | 86.7 | 88.0 | 90.1 |

and $l * h_D$ features for X_D , respectively. These two feature vectors are further combined into a single vector of length $l * (m + h_D)$ ($= 186$). For both architectures, kNN classification was applied for final class prediction using as distance measure between two feature vectors, x_1 and x_2 , the metric $1 - \text{cor}(x_1, x_2)$, where cor is the sample Spearman's rank correlation. The value $k = 12$ was selected for all experiments. For comparison, fusion was also performed with linear SVM classification ([Chang & Lin, 2011](#)). The code was developed in MATLAB environment and the implementation of CNNs was based on MatConvNet ([Vedaldi & Lenc, 2015](#)).

RESULTS

The protein structures ($n = 44,661$) were collected from the PDB. Only enzymes that occur in a single class were processed, whereas enzymes that perform multiple reactions and are hence associated with multiple enzymatic functions were excluded. Since protein sequence was not examined during feature extraction, all enzymes were considered without other exclusion criteria, such as small sequence length or homology bias. The dataset was unbalanced in respect to the different classes. The number of samples per class is shown in [Table 1](#). The dataset was split into five folds. Four folds were used for training and one for testing. The training samples were used to learn the parameters of the network (such as the weights of the convolution filters), as well as the parameters of the subsequent classifiers used during fusion (SVM or kNN model). Once the network was trained, the class probabilities were obtained for the testing samples, which were introduced into the trained SVM or kNN classifier for final prediction. The SVM model was linear and thus didn't require any hyper-parameter optimization. Due to the lack of hyper-parameters, no extra validation set was necessary. On the side, the author also examined non-linear SVM with a Gaussian radial basis function kernel, but didn't observe any significant improvement; thus, the corresponding results are not reported.

A classification result was deemed a true positive if the match with the highest probability was in first place in a rank-ordered list. The classification accuracy (percentage of correctly classified samples over all samples) was calculated for each fold and then averaged across the five folds.

Table 2 Confusion matrices for each fusion scheme and classification technique.

| Classifier | | Prediction by <i>Architecture 1</i> | | | | | | Prediction by <i>Architecture 2</i> | | | | | |
|------------|-----|-------------------------------------|-------------|-------------|-------------|-------------|-------------|-------------------------------------|-------------|-------------|-------------|-------------|-------------|
| | | 1 | 2 | 3 | 4 | 5 | 6 | 1 | 2 | 3 | 4 | 5 | 6 |
| Linear-SVM | EC1 | 86.5 | 4.9 | 4.8 | 1.8 | 1.1 | 1.0 | 91.2 | 2.9 | 1.9 | 2.2 | 1.1 | 0.7 |
| | EC2 | 3.4 | 84.0 | 7.9 | 1.9 | 1.2 | 1.6 | 3.6 | 88.0 | 3.5 | 2.2 | 1.2 | 1.5 |
| | EC3 | 2.4 | 6.1 | 88.7 | 1.0 | 0.8 | 1.0 | 2.3 | 4.1 | 89.6 | 1.6 | 1.2 | 1.2 |
| | EC4 | 4.4 | 7.3 | 5.7 | 79.4 | 1.8 | 1.3 | 4.3 | 4.9 | 2.7 | 84.9 | 1.7 | 1.4 |
| | EC5 | 7.0 | 10.1 | 9.0 | 2.9 | 69.4 | 1.6 | 4.5 | 5.4 | 4.7 | 4.4 | 79.5 | 1.7 |
| | EC6 | 5.9 | 15.5 | 13.0 | 2.3 | 2.3 | 61.0 | 5.5 | 10.3 | 5.4 | 3.3 | 1.9 | 73.6 |
| kNN | EC1 | 88.8 | 5.0 | 4.5 | 0.7 | 0.5 | 0.5 | 90.6 | 4.4 | 4.6 | 0.3 | 0.1 | 0.0 |
| | EC2 | 2.5 | 87.5 | 7.4 | 1.0 | 0.6 | 1.1 | 1.7 | 91.7 | 5.8 | 0.3 | 0.2 | 0.4 |
| | EC3 | 1.8 | 5.4 | 91.3 | 0.5 | 0.4 | 0.6 | 1.2 | 4.4 | 94.0 | 0.2 | 0.1 | 0.2 |
| | EC4 | 3.8 | 9.1 | 7.2 | 78.5 | 1.1 | 0.4 | 3.7 | 8.4 | 6.9 | 80.7 | 0.1 | 0.1 |
| | EC5 | 6.1 | 11.5 | 10.7 | 2.3 | 68.5 | 1.0 | 3.5 | 9.7 | 8.6 | 0.9 | 76.9 | 0.3 |
| | EC6 | 4.9 | 18.8 | 13.5 | 1.0 | 1.3 | 60.6 | 4.2 | 14.1 | 10.3 | 0.7 | 0.3 | 70.5 |

Classification performance

Common options for the network were used, except of the size of the filters which was adjusted to the dimensionality of the input data. Specifically, the convolutional layer used neurons with a receptive field of size 5 for the first two layers and 2 for the third layer. The stride (specifying the sliding of the filter) was always 1. The number of filters was 20, 50 and 500 for the three layers, respectively, and the learning rate was 0.001. The batch size was selected according to the information amount (dimensionality) of the input. It was assumed (and verified experimentally) that for more complicated data, a larger number of samples is required for learning. One thousand samples per batch were used for *Architecture 1*, which takes as input all channels, and 100 samples per batch for *Architecture 2*, in which an independent CNN is trained for each channel. The dropout rate was 20%. The number of epochs was adjusted to the rate of convergence for each architecture (300 for *Architecture 1* and 150 for *Architecture 2*).

The average classification accuracy over the five folds for each enzymatic class is shown in [Table 1](#) for both fusion schemes, whereas the analytic distribution of samples in each class is shown in the form of confusion matrices in [Table 2](#).

In order to further assess the performance of the deep networks, receiver operating characteristic (ROC) curves and area-under-the-curve (AUC) values were calculated for each class for the selected scheme (based on kNN and *Architecture 2*), as shown in [Fig. 2](#)). The calculations were performed based on the final decision scores in a one-versus-rest classification scheme. The decision scores for the kNN classifier reflected the ratio of the within-class neighbors over total number of neighbors. The ROC curve represents the true positive rate against the false positive rate and was produced by averaging over the five folds of the cross-validation experiments.

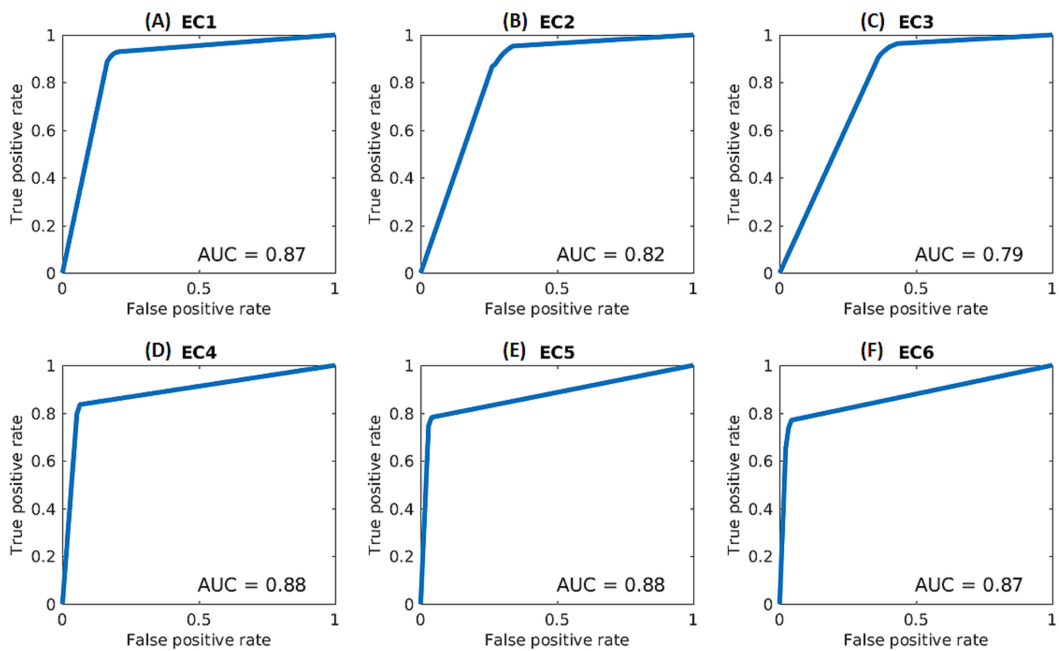


Figure 2 ROC curves for each enzymatic class based on kNN and *Architecture 2*. (A) EC1, (B) EC2, (C) EC3, (D) EC4, (E) EC5, (F) EC6.

Effect of sequence redundancy and sample size

Analysis of protein datasets is often performed after removal of redundancy, such that the remaining entries do not overreach a pre-arranged threshold of sequence identity. In the previously presented results, sequence/threshold metrics were not applied to remove sequence-redundancy. Although structure similarity is affected by sequence similarity, the aim was not to lose structural entries (necessary for efficient learning) over a sequence based threshold cutoff. Also, only X-ray crystallography data were used; such data represent a ‘snapshot’ of a given protein’s 3D structure. In order not to miss the multiple poses that the same protein may adopt in different crystallography experiments, the whole dataset was explored.

Subsequently, the performance of the method was also investigated on a less redundant dataset and the classification accuracy was compared in respect to the original (redundant) dataset, but randomly subsampled to include equal number of proteins. This experiment allows to assess the effect of redundancy under the same conditions (number of samples). Since inference in deep networks requires the estimation of a very large number of parameters, a large amount of training data is required and therefore very strict filtering strategies could not be applied. A dataset, the *pdbaanr* (http://dunbrack.fccc.edu/Guoli/pisces_download.php), pre-compiled by PISCES (Wang & Dunbrack, 2003), was used that includes only non-redundant sequences across all PDB files ($n = 23242$ proteins, i.e., half in size of the original dataset). This dataset has one representative for each unique sequence in the PDB; representative chains are selected based on the highest resolution structure available and then the best R -values. Non-X-ray structures are considered after X-ray structures. As a note, the author also explored the

Leaf algorithm (Bull, Muldoon & Doig, 2013) which is especially designed to maximize the number of retained proteins and has shown improvement over PISCES. However, the computational cost was too high (possibly due to the large number of samples) and the analysis was not completed.

The classification performance was assessed on *Architecture 2* by using 80% of the samples for training and 20% of the samples for testing. For the *pdbaanr* dataset, the accuracy was 79.3% for kNN and 75.5% for linear-SVM, whereas for the sub-sampled dataset it was 85.7% for kNN and 83.2% for linear-SVM. The results show that for the selected classifier (kNN), the accuracy drops 4.4% when the number of samples is reduced to the half, and it also drops additionally 6.4% if the utilized sequences are less similar. The decrease in performance shows that the method is affected by the number of samples as well as by their similarity level.

Structural representation and complementarity of features

Next, some examples of the extracted feature maps are illustrated, in order to provide some insight on the representation of protein's 3D structure. The average (over all samples) 2D histogram of torsion angles for each amino acid is shown in [Fig. 3](#). The horizontal and vertical axes at each plot represent torsion angles (in $[-180^\circ, 180^\circ]$). It can be observed that the non-standard (ASX, GLX, UNK) amino acids are very rare, thus their density maps have mostly zeros. The same color scale was used in all plots to make feature maps comparable, as “seen” by the deep network. Since the histograms are (deliberately) not normalized for each sample, rare amino acids will have few visible features and due to the ‘max-pooling operator’ will not be selected as significant features. The potential of these feature maps to differentiate between classes is illustrated in [Fig. 4](#) for three randomly selected amino acids (ALA, GLY, TYR). Overall the spatial patterns in each class are distinctive and form a multi-dimensional signature for each sample. As a note, before training of the CNN ensemble, data standardization is performed by subtracting the mean density map. The same map is used to standardize the test sample during assessment.

Examples of features maps representing amino acid distances (X_D) are illustrated in [Figs. 1](#) and [5](#). [Figure 1](#) illustrates an image slice across the 3rd dimension, i.e., one $[m \times m]$ channel, and as introduced in the 2D multichannel CNN, i.e., after mean-centering (over all samples). [Figure 5](#) illustrates image slices (of size $[m \times h_D]$) across the 1st dimension averaged within each class. [Figure 5](#) has been produced by selecting the same amino acids as in [Fig. 4](#) for ease of comparison of the different feature representations. It can be noticed that for all classes most pairwise distances are concentrated in the last bin, corresponding to high distances between amino acids. Also, as expected there are differences in quantity of each amino acid, e.g., by focusing on the last bin, it can be seen that ALA and GLY have higher values than TYR in most classes. Moreover, the feature maps indicate clear differences between samples of different classes.

The discrimination ability and complementarity of the extracted features in respect to classification performance is shown in [Table 3](#). It can be observed that the relative position of amino acids and their arrangement in space (features X_D) predict enzymatic function better than the backbone conformation (features X_A). Also, the fusion of network decisions

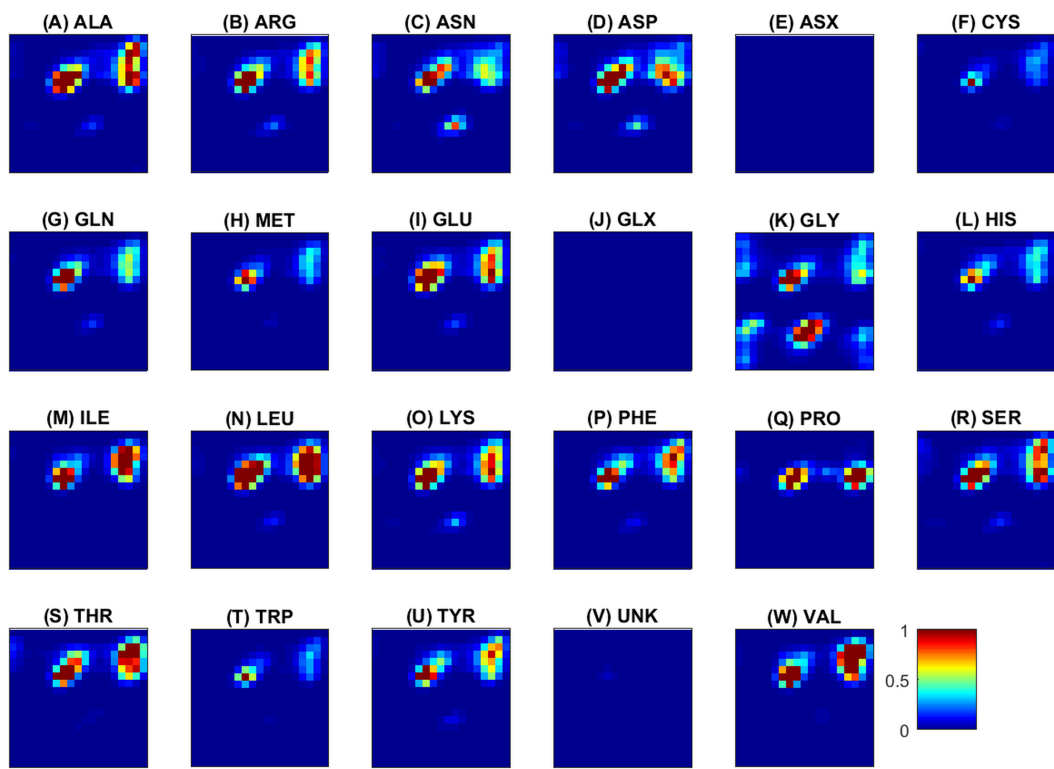


Figure 3 Torsion angles density maps (Ramachandran plots) averaged over all samples for each of the 20 standard and three non-standard (ASX, GLX, UNK) amino acids shown in alphabetical order from (A) to (W). The horizontal and vertical axes at each plot correspond to ϕ and ψ angles and vary from -180° (top left) to 180° (right bottom). The color scale (blue to red) is in the range [0, 1]. For an amino acid a , red means that the number of occurrences of the specific value (ϕ, ψ) in all observations of a (within and across proteins) is at least equal to the number of proteins. On the opposite, blue indicates a small number of occurrences, and is observed for rare amino acids or unfavorable conformations. (A) ALA, (B) ARG, (C) ASN, (D) ASP, (E) ASX, (F) CYS, (G) GLN, (H) MET, (I) GLU, (J) GLX, (K) GLY, (L) HIS, (M) ILE, (N) LEU, (O) LYS, (P) PHE, (Q) PRO, (R) SER, (S) THR, (T) TRP, (U) TYR, (V) UNK, (W) VAL.

Table 3 Cross-validation accuracy (average \pm standard deviation over five folds) for each feature set separately and after fusion of CNN outputs based on *Architecture 2*.

| Feature sets | Linear-SVM | kNN |
|-------------------|----------------|----------------|
| X_A (angles) | 79.6 ± 0.5 | 82.4 ± 0.4 |
| X_D (distances) | 88.1 ± 0.4 | 89.8 ± 0.2 |
| Ensemble | 88.0 ± 0.4 | 90.1 ± 0.2 |

based on correlation distance outperforms predictions from either network alone, but the difference is only marginal in respect to the predictions by X_D . In all cases the differences in prediction for the performed experiments (during cross validation) was very small (usually standard deviation $< 0.5\%$), indicating that the method is robust to variations in training examples.

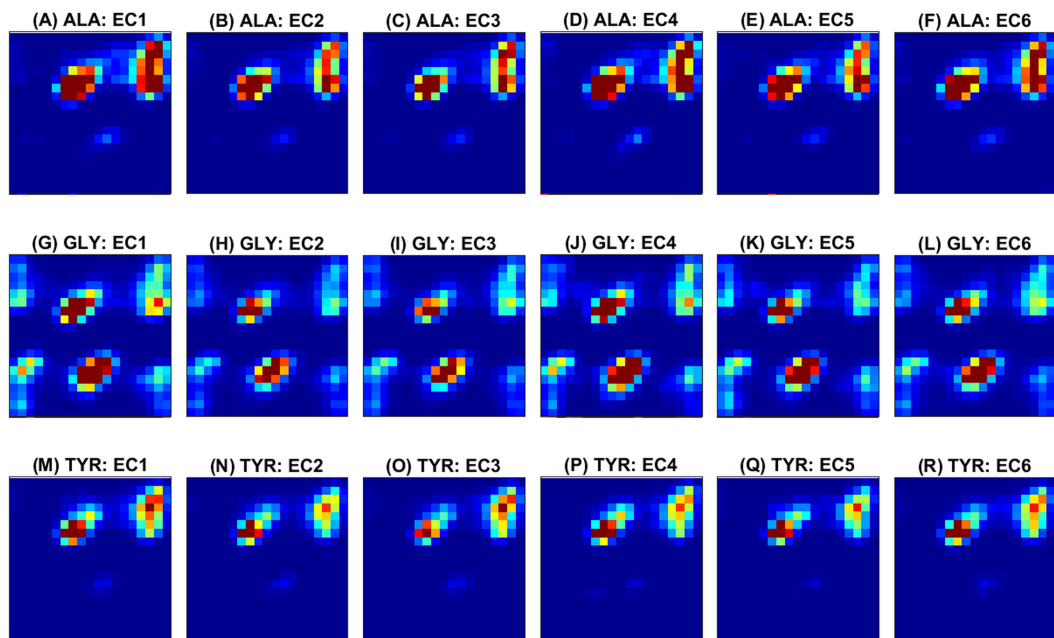


Figure 4 Ramachandran plots averaged across samples within each class. Rows correspond to amino acids and columns to functional classes. Three amino acids (ALA from (A) to (F), GLY from (G) to (L) and TYR from (M) to (R)) are randomly selected for illustration of class separability. The horizontal and vertical axes at each plot correspond to ϕ and ψ angles and vary from -180° (top left) to 180° (right bottom). The color scale (blue to red) is in the range [0, 1] as illustrated in Fig. 3.

DISCUSSION

A deep CNN ensemble was presented that performs enzymatic function classification through fusion in feature level and decision level. The method has been applied for the prediction of the primary EC number and achieved 90.1% accuracy, which is a considerable improvement over the accuracy obtained in our previous work (73.5% in [Amidi et al. \(2016\)](#) and 83% in [Amidi et al. \(2017\)](#)) when only structural information was incorporated. These results were achieved without imposing any pre-selection criteria, such as based on sequence identity, thus the effect of evolutionary relationships, as confounding factor in the prediction of function from 3D structure, has not been sufficiently studied. Since deep learning technology requires a large number of samples to produce generalizable models, a filtered dataset with only non-redundant proteins would be too small for reliable training. This is a limitation of the current approach, which mainly aimed to increase predictive power over previous methods using common features for structural representation and common classifiers such as SVM and nearest neighbor, rather than addressing this confounding factor in the prediction of protein structure.

Many methods have been proposed in the literature using different features and different classifiers. [Nasibov & Kandemir-Cavas \(2009\)](#) obtained 95%–99% accuracy by applying kNN-based classification on 1200 enzymes based on their amino acid composition. [Shen & Chou \(2007\)](#) fused results derived from the functional domain and evolution information and obtained 93.7% average accuracy on 9,832 enzymes. On the same dataset,

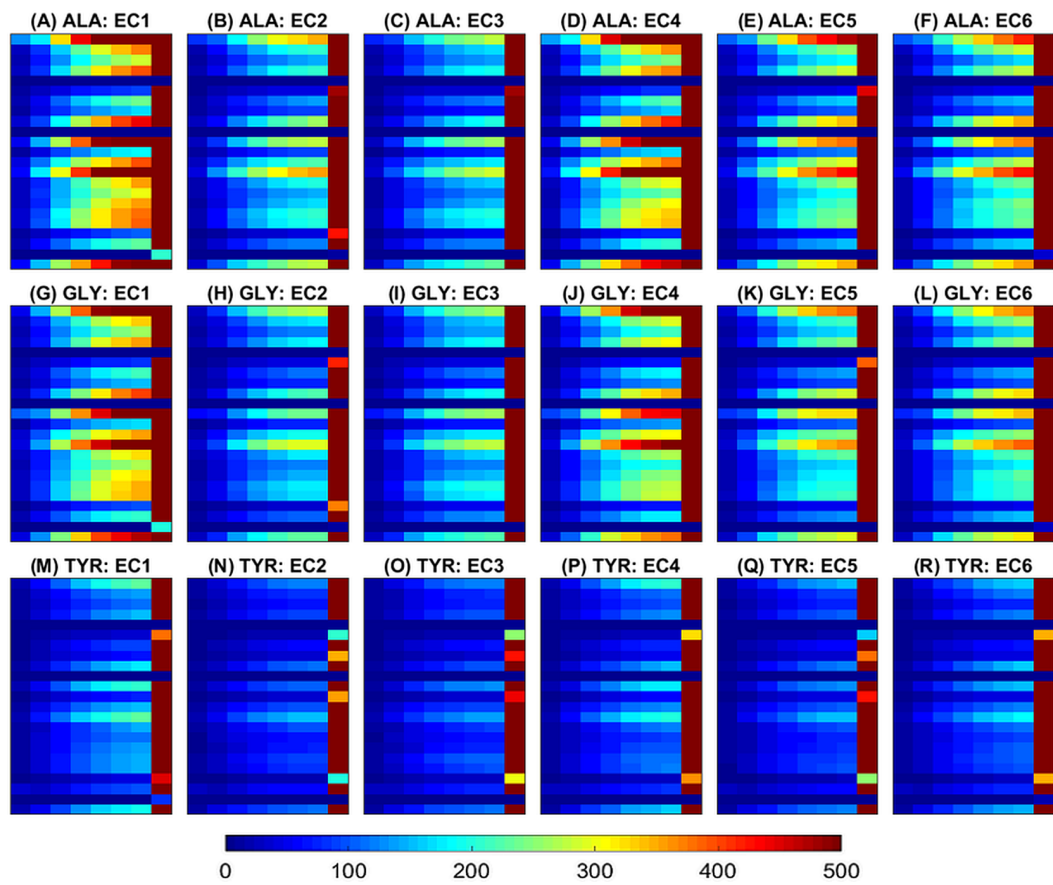


Figure 5 Histograms of pairwise amino acid distances averaged across samples within each class. The same three amino acids selected in Fig. 4 are also shown here (ALA from (A) to (F), GLY from (G) to (L) and TYR from (M) to (R)). The horizontal axis at each plot represents the histogram bins (distance values in the range [5, 40]). The vertical axis at each plot corresponds to the 23 amino acids sorted alphabetically from top to bottom (ALA, ARG, ASN, ASP, ASX, CYS, GLN, MET, GLU, GLX, GLY, HIS, ILE, LEU, LYS, PHE, PRO, SER, THR, TRP, TYR, UNK, VAL). Thus each row shows the histogram of distances for a specific pair of the amino acids (the one in the title and the one corresponding to the specific row). The color scale is the same for all plots and is shown horizontally at the bottom of the figure.

[Wang et al. \(2011\)](#) improved the accuracy (which ranged from 81% to 98% when predicting the first three EC digits) by using sequence encoding and SVM for hierarchy labels. [Kumar & Choudhary \(2012\)](#) reported overall accuracy of 87.7% in predicting the main class for 4,731 enzymes using random forests. [Volpato, Adelfio & Pollastri \(2013\)](#) applied neural networks on the full sequence and achieve 96% correct classification on 6,000 non-redundant proteins. Most of the previous methods incorporate sequence-based features. Many were assessed on a subset of enzymes acquired after imposition of different pre-selection criteria and levels of sequence similarity. More discussion on machine learning techniques for single-label and multi-label enzyme classification can be found in [Amidi et al. \(2017\)](#).

Assessment of the relationship between function and structure ([Todd, Orengo & Thornton, 2001](#)) revealed 95% conservation of the fourth EC digit for proteins with up to 30% sequence identity. Similarity, [Devos & Valencia \(2000\)](#) concluded that enzymatic

function is mostly conserved for the first digit of EC code whereas more detailed functional characteristics are poorly conserved. It is generally believed that as sequences diverge, 3D protein structure becomes a more reliable predictor than sequence, and that structure is far more conserved than sequence in nature (Illegård, Ardel & Elofsson, 2009). The focus of this study was to explore the predictive ability of 3D structure and provide a tool that can generalize in cases where sequence information is insufficient. Thus, the presented results are not directly comparable to the ones of previous methods due to the use of different features and datasets. If desired, the current approach can easily incorporate also sequence-related features. In such a case however, the use of non-homologous data would be inevitable for rigorous assessment.

The reported accuracy is the average of five folds on the testing set. A separate validation set was not used within each fold, because the design of the network architecture (size of convolution kernel, number of layers, etc.) and the final classifier (number of neighbors in kNN) were preselected and not optimized within the learning framework. Additional validation and optimization of the model would be necessary to improve performance and provide better insight into the capabilities of this method.

A possible limitation of the proposed approach is that the extracted features do not capture the topological properties of the 3D structure. Due to the statistical nature of the implemented descriptors, which were calculated by considering the amino acids as elements in Euclidean space, connectivity information is not strictly retained. The author and colleagues recently started to investigate in parallel the predictive power of the original 3D structure, represented as a volumetric image, without the extraction of any statistical features. Since the more detailed representation increased the dimensionality considerably, new ways are being explored to optimally incorporate the relationship between the structural units (amino-acids) in order not to impede the learning process.

CONCLUSIONS

A method was presented that extracts shape features from the 3D protein geometry that are introduced into a deep CNN ensemble for enzymatic function prediction. The investigation of protein function based only on structure reveals relationships hidden at the sequence level and provides the foundation to build a better understanding of the molecular basis of biological complexity. Overall, the presented approach can provide quick protein function predictions on extensive datasets opening the path for relevant applications, such as pharmacological target identification. Future work includes application of the method for prediction of the hierarchical relation of function subcategories and annotation of enzymes up to the last digit of the enzyme classification system.

ACKNOWLEDGEMENTS

The authors want to thank Prof. N Paragios from the Center for Visual Computing, CentraleSupélec, Paris, for providing the means to complete this study and Dr. D Vlachakis from the Multidimensional Data Analysis and Knowledge Management Laboratory, University of Patras, for useful discussions on the biological aspects.

ADDITIONAL INFORMATION AND DECLARATIONS

Funding

This research was partially supported by European Research Council Grant Diocles (ERC-STG-259112). There was no additional external funding received for this study. The funders had no role in study design, data collection and analysis, decision to publish, or preparation of the manuscript.

Grant Disclosures

The following grant information was disclosed by the author:
European Research Council Grant Diocles: ERC-STG-259112.

Competing Interests

The authors declare there are no competing interests.

Author Contributions

- Evangelia I. Zacharaki conceived and designed the experiments, performed the experiments, analyzed the data, wrote the paper, prepared figures and/or tables, performed the computation work, reviewed drafts of the paper.

Data Availability

The following information was supplied regarding data availability:

The raw data can be found in the PDB public database: www.rcsb.org/pdb/. The code can be downloaded from <https://github.com/ezachar/PeerJ>. The code can run either using PDB entries downloaded locally or by accessing the entries from the PDB during run-time.

REFERENCES

- Amidi A, Amidi S, Vlachakis D, Paragios N, Zacharaki EI.** 2016. A machine learning methodology for enzyme functional classification combining structural and protein sequence descriptors. In: *Bioinformatics and Biomedical Engineering*. Cham: Springer, 728–738.
- Amidi S, Amidi A, Vlachakis D, Paragios N, Zacharaki EI.** 2017. Automatic single- and multi-label enzymatic function prediction by machine learning. *PeerJ* 5:e3095 DOI [10.7717/peerj.3095](https://doi.org/10.7717/peerj.3095).
- Bermejo GA, Clore GM, Schwieters CD.** 2012. Smooth statistical torsion angle potential derived from a large conformational database via adaptive kernel density estimation improves the quality of NMR protein structures. *Protein Science* 21(12):1824–1836 DOI [10.1002/pro.2163](https://doi.org/10.1002/pro.2163).
- Borgwardt KM, Ong CS, Schönauer S, Vishwanathan S, Smola AJ, Kriegel H-P.** 2005. Protein function prediction via graph kernels. *Bioinformatics* 21(suppl 1):i47–i56 DOI [10.1093/bioinformatics/bti1007](https://doi.org/10.1093/bioinformatics/bti1007).
- Borro LC, Oliveira SR, Yamagishi ME, Mancini AL, Jardine JG, Mazoni I, Santos ED, Higa RH, Kuser PR, Neshich G.** 2006. Predicting enzyme class from protein structure using Bayesian classification. *Genetics and Molecular Research* 5(1):193–202.

- Bull SC, Muldoon MR, Doig AJ. 2013.** Maximising the size of non-redundant protein datasets using graph theory. *PLOS ONE* 8(2):e55484
[DOI 10.1371/journal.pone.0055484](https://doi.org/10.1371/journal.pone.0055484).
- Cai C, Han L, Ji ZL, Chen X, Chen YZ. 2003.** SVM-Prot: web-based support vector machine software for functional classification of a protein from its primary sequence. *Nucleic Acids Research* 31(13):3692–3697 [DOI 10.1093/nar/gkg600](https://doi.org/10.1093/nar/gkg600).
- Chang C-C, Lin C-J. 2011.** LIBSVM: a library for support vector machines. *ACM Transactions on Intelligent Systems and Technology (TIST)* 2(3):Article 27
[DOI 10.1145/1961189.1961199](https://doi.org/10.1145/1961189.1961199).
- Chen C, Tian Y-X, Zou X-Y, Cai P-X, Mo J-Y. 2006.** Using pseudo-amino acid composition and support vector machine to predict protein structural class. *Journal of Theoretical Biology* 243(3):444–448 [DOI 10.1016/j.jtbi.2006.06.025](https://doi.org/10.1016/j.jtbi.2006.06.025).
- Devos D, Valencia A. 2000.** Practical limits of function prediction. *Proteins: Structure, Function, and Bioinformatics* 41(1):98–107
[DOI 10.1002/1097-0134\(20001001\)41:1<98::AID-PROT120>3.0.CO;2-S](https://doi.org/10.1002/1097-0134(20001001)41:1<98::AID-PROT120>3.0.CO;2-S).
- Dobson PD, Doig AJ. 2005.** Predicting enzyme class from protein structure without alignments. *Journal of Molecular Biology* 345(1):187–199
[DOI 10.1016/j.jmb.2004.10.024](https://doi.org/10.1016/j.jmb.2004.10.024).
- Godzik A. 2011.** Metagenomics and the protein universe. *Current Opinion in Structural Biology* 21(3):398–403 [DOI 10.1016/j.sbi.2011.03.010](https://doi.org/10.1016/j.sbi.2011.03.010).
- Han L, Cai C, Ji Z, Cao Z, Cui J, Chen Y. 2004.** Predicting functional family of novel enzymes irrespective of sequence similarity: a statistical learning approach. *Nucleic Acids Research* 32(21):6437–6444 [DOI 10.1093/nar/gkh984](https://doi.org/10.1093/nar/gkh984).
- Huang W-L, Chen H-M, Hwang S-F, Ho S-Y. 2007.** Accurate prediction of enzyme subfamily class using an adaptive fuzzy k-nearest neighbor method. *Biosystems* 90(2):405–413 [DOI 10.1016/j.biosystems.2006.10.004](https://doi.org/10.1016/j.biosystems.2006.10.004).
- Illergård K, Ardell DH, Elofsson A. 2009.** Structure is three to ten times more conserved than sequencea study of structural response in protein cores. *Proteins: Structure, Function, and Bioinformatics* 77(3):499–508 [DOI 10.1002/prot.22458](https://doi.org/10.1002/prot.22458).
- Krizhevsky A, Sutskever I, Hinton GE. 2012.** Imagenet classification with deep convolutional neural networks. In: *Advances in Neural Information Processing Systems*. 1097–1105.
- Kumar C, Choudhary A. 2012.** A top-down approach to classify enzyme functional classes and sub-classes using random forest. *EURASIP Journal on Bioinformatics and Systems Biology* 2012(1):1–14 [DOI 10.1186/1687-4153-2012-1](https://doi.org/10.1186/1687-4153-2012-1).
- Lee BJ, Shin MS, Oh YJ, Oh HS, Ryu KH. 2009.** Identification of protein functions using a machine-learning approach based on sequence-derived properties. *Proteome Science* 7:1 [DOI 10.1186/1477-5956-7-1](https://doi.org/10.1186/1477-5956-7-1).
- Li Y, Shibuya T. 2015.** Malphite: a convolutional neural network and ensemble learning based protein secondary structure predictor. In: *IEEE International conference on bioinformatics and biomedicine (BIBM)*. Piscataway: IEEE, 1260–1266.

- Lin Z, Lanchantin J, Qi Y. 2016.** MUST-CNN: a multilayer shift-and-stitch deep convolutional architecture for sequence-based protein structure prediction. In: *30th AAAI conference on artificial intelligence*. Menlo Park: AAAI.
- Lu L, Qian Z, Cai Y-D, Li Y. 2007.** ECS: an automatic enzyme classifier based on functional domain composition. *Computational Biology and Chemistry* **31**(3):226–232 DOI [10.1016/j.combiolchem.2007.03.008](https://doi.org/10.1016/j.combiolchem.2007.03.008).
- Nagao C, Nagano N, Mizuguchi K. 2014.** Prediction of detailed enzyme functions and identification of specificity determining residues by random forests. *PLOS ONE* **9**(1):1–12 DOI [10.1371/journal.pone.0084623](https://doi.org/10.1371/journal.pone.0084623).
- Nasibov E, Kandemir-Cavas C. 2009.** Efficiency analysis of KNN and minimum distance-based classifiers in enzyme family prediction. *Computational Biology and Chemistry* **33**(6):461–464 DOI [10.1016/j.combiolchem.2009.09.002](https://doi.org/10.1016/j.combiolchem.2009.09.002).
- Qiu J-D, Huang J-H, Shi S-P, Liang R-P. 2010.** Using the concept of Chou's pseudo amino acid composition to predict enzyme family classes: an approach with support vector machine based on discrete wavelet transform. *Protein and Peptide Letters* **17**(6):715–722 DOI [10.2174/092986610791190372](https://doi.org/10.2174/092986610791190372).
- Sharma M, Garg P. 2014.** Computational approaches for enzyme functional class prediction: a review. *Current Proteomics* **11**(1):17–22 DOI [10.2174/1570164611666140415225013](https://doi.org/10.2174/1570164611666140415225013).
- Shen H-B, Chou K-C. 2007.** EzyPred: a top-down approach for predicting enzyme functional classes and subclasses. *Biochemical and Biophysical Research Communications* **364**(1):53–59 DOI [10.1016/j.bbrc.2007.09.098](https://doi.org/10.1016/j.bbrc.2007.09.098).
- Spencer M, Eickholt J, Cheng J. 2015.** A deep learning network approach to ab initio protein secondary structure prediction. *IEEE/ACM transactions on computational biology and bioinformatics (TCBB)* **12**(1):103–112 DOI [10.1109/TCBB.2014.2343960](https://doi.org/10.1109/TCBB.2014.2343960).
- Todd AE, Orengo CA, Thornton JM. 2001.** Evolution of function in protein superfamilies, from a structural perspective. *Journal of Molecular Biology* **307**(4):1113–1143 DOI [10.1006/jmbi.2001.4513](https://doi.org/10.1006/jmbi.2001.4513).
- Vedaldi A, Lenc K. 2015.** Matconvnet: convolutional neural networks for MATLAB. In: *Proceedings of the 23rd ACM international conference on multimedia*. New York: ACM, 689–692.
- Volpatto V, Adelfio A, Pollastri G. 2013.** Accurate prediction of protein enzymatic class by n-to-1 neural networks. *BMC Bioinformatics* **14**(1):1 DOI [10.1186/1471-2105-14-1](https://doi.org/10.1186/1471-2105-14-1).
- Wang G, Dunbrack RL. 2003.** PISCES: a protein sequence culling server. *Bioinformatics* **19**(12):1589–1591 DOI [10.1093/bioinformatics/btg224](https://doi.org/10.1093/bioinformatics/btg224).
- Wang Y-C, Wang X-B, Yang Z-X, Deng N-Y. 2010.** Prediction of enzyme subfamily class via pseudo amino acid composition by incorporating the conjoint triad feature. *Protein and Peptide Letters* **17**(11):1441–1449 DOI [10.2174/0929866511009011441](https://doi.org/10.2174/0929866511009011441).
- Wang Y-C, Wang Y, Yang Z-X, Deng N-Y. 2011.** Support vector machine prediction of enzyme function with conjoint triad feature and hierarchical context. *BMC Systems Biology* **5**(1):1 DOI [10.1186/1752-0509-5-1](https://doi.org/10.1186/1752-0509-5-1).

- Webb EC.** 1992. Enzyme nomenclature 1992. In: *Recommendations of the nomenclature committee of the international union of biochemistry and molecular biology on the nomenclature and classification of enzymes*. San Diego: Academic Press.
- Yadav SK, Tiwari AK.** 2015. Classification of enzymes using machine learning based approaches: a review. *Machine Learning and Applications* 2(3/4):30–49.
- Zhou X-B, Chen C, Li Z-C, Zou X-Y.** 2007. Using Chou's amphiphilic pseudo-amino acid composition and support vector machine for prediction of enzyme subfamily classes. *Journal of Theoretical Biology* 248(3):546–551 DOI [10.1016/j.jtbi.2007.06.001](https://doi.org/10.1016/j.jtbi.2007.06.001).